Numerical simulation of bone screw induced pretension: The cases of under-tapping and conical profile

3 authors:

Panagiotis Chatzistergos
Staffordshire University
53 PUBLICATIONS   113 CITATIONS

SEE PROFILE

Evangelos A Magnissalis
39 PUBLICATIONS   231 CITATIONS

SEE PROFILE

Stavros Kourkoulis
National Technical University of Athens
134 PUBLICATIONS   570 CITATIONS

SEE PROFILE

Some of the authors of this publication are also working on these related projects:

Project

DiaBSmart: Development of a new generation of DIABetic footwear using an integrated approach and SMART materials View project

NUMERICAL SIMULATION OF BONE SCREW INDUCED PRETENSION: THE CASES OF UNDER-TAPPING AND CONICAL PROFILE.

Panagiotis E. Chatzistergos [(1),(*)], Evangelos A. Magnissalis [(2)] and

Stavros K. Kourkoulis [(3)]

(1)   Faculty of Health Sciences, Staffordshire University, Science Centre, Leek Road, ST4 2DF, Stoke on Trent, Staffordshire, UK

(2)   BioHexagon LTD, Varnis 36, Nea Smyrni, Attiki, Greece

(3)   Unit of Biomechanics, Department of Mechanics, School of Applied Mathematical and Physical Sciences, National Technical University of Athens, Zografou Campus, Theocaris building, 157-73 Attiki, Greece

(*)   Corresponding author, tel.: +44 1782 295920

      e-mail: panagiotis.chatzistergos@staffs.ac.uk

25 **Abstract:**

26 Even though screw induced pretension impacts the holding strength of bone screws,

27 its implementation into the numerical simulation of the pullout phenomenon remains

28 a problem with no apparent solution. The present study aims at developing a new

29 methodology to simulate screw induced pretension for the cases of: a) cylindrical

30 screws inserted with under-tapping and b) conical screws. For this purpose pullout

31 was studied experimentally using synthetic bone and then simulated numerically.

32 Synthetic bone failure was simulated using a bilinear cohesive zone material model.

33 Pretension generation was simulated by allowing the screw to expand inside a hole

34 with smaller dimensions or different shape than the screw itself. The finite element

35 models developed here were validated against experimental results and then utilized

36 to investigate the impact of under-tapping and conical angle. The results indicated that

37 pretension can indeed increase a screw's pullout force but only up to a certain degree.

38 Under-tapping increased cylindrical screws' pullout force up to 12%, 15% and 17%

39 for synthetic bones of density equal to 0.08 g/cc, 0.16 g/cc and 0.28 g/cc respectively.

40 Inserting a conical screw into a cylindrical hole increased pullout force up to 11%. In

41 any case an optimum level of screw induced pretension exists.

42

43

44

47

48

49

2

1.   Introduction

Despite the extensive use of pedicle screws and the significant advances in the field of spinal stabilization the possibility of screw loosening and pullout remains and is even higher in the case of osteoporotic patients [1-3].

There are strong indications in the literature that the pretension developed in the vicinity of bone screws during their insertion can significantly influence their pullout strength. Experimental studies performed on synthetic [4] or cadaveric [5, 6] bone specimens showed that the holding strength of a cylindrical screw can be improved by under-tapping; namely by inserting the screw into a cylindrical threaded hole which is smaller than the screw itself. Screw insertion with under-tapping causes the core diameter of the threaded hole to expand and the screw hosting material in the vicinity of the screw to compact. In this case the screw's hosting material is compacted uniformly along the length of the screw.

In a previous experimental investigation [4] performed by authors of the present study, it was found that using a tap that is one size smaller than the screw, can increase the pullout force by 9%. Further reduction of the threaded hole dimensions did not result in any statistically significant change of the pullout force.

A combined experimental and numerical analysis of the pullout behaviour of cylindrical self tapping screws was performed by Wu et al. [7]. The authors of this study designed an axisymmetric finite element (FE) model of a screw that is inserted into a threaded hole with dimensions and shape identical to the screw itself. The pretension generated during screw insertion was simulated by introducing a

3

75 temperature change. Even though their model appears to be capable of generating an

76 initial pretension inside the screw's hosting material, the way this capability was

77 utilized is not clear. Numerical results are presented only for cases where the radius of

78 the pilot hole is equal to the screw's core radius.

79

80 Moreover, screws with conical core were found to have higher pullout strengths than

81 cylindrical screws with similar thread shape and size [8-13]. Screws with conical core

82 are inserted into cylindrical holes with diameters smaller than the maximum core

83 diameter of the screw. In this case, screw insertion results in a non-uniform

84 compaction of the screw's hosting material. Indeed the screw's hosting material that is

85 closer to the screw's entry site is compacted more than that closer to the screw's tip.

86

87 In a previous attempt to simulate the effect of bone compaction in the vicinity of a

88 conical screw that is inserted into a cylindrical hole, the elastic modulus of the screw's

89 hosting material was modified based on an estimate of its volume reduction [8, 9].

90 The main disadvantage of this approach is that the effect of bone compaction is

91 predefined.

92

93 Another interesting approach to the numerical simulation of the pretension that is

94 developed in the vicinity of an implant was presented by Janssen et al. [14] for the

95 case of press-fit acetabular implants. The authors of this study simulated the insertion

96 of the implant as a separate load step.

97

98 Considering all the above, the present study aims at developing a reliable and accurate

99 technique to integrate the screw induced pretension to the numerical simulation of the

100   pullout phenomenon. The accuracy of the numerical analyses performed here was

101   assessed by comparing numerical and experimental results for four different screw

102   insertion scenarios.

103

104   One of the key features for the numerical assessment of a screw's pullout strength is

105   the simulation of the screw's hosting material failure [7, 15-17]. For the purpose of the

106   present study the failure of the screw's hosting material was simulated using a bilinear

107   cohesive zone material model [15, 18]. The validity of this technique for the

108   simulation of screw pullout has been previously established for cylindrical screws that

109   are inserted into blocks of synthetic bone without any pretension [15]. Its accuracy

110   has also been validated for different densities of synthetic bone [19].

111

112

113   **2.   Materials and methods**

114

115   2.1   Experimental study

116   Pullout tests were performed with the use of solid rigid polyurethane foam (SRPF)

117   blocks with density equal to 0.16 g/cc and material properties similar to osteoporotic

118   cancellous bone (10 pcf SRPF, Sawbones, Worldwide, Pacific Research Laboratories

119   Inc.) and two commercially available pedicle screws, namely Romeo® polyaxial

120   screws for lumbar fixation (Spineart, International Center Cointrin, Genève, Suisse).

121   The two screws used for the completion of the pullout tests are shown in figure 1. As

122   it can be seen, their thread can be divided into two parts of similar lengths: a

123   cylindrical one and a conical one ($L_{con} = L_{cyl} \approx 20$ mm). The main geometrical

124   features of the aforementioned screws are shown in figure 1 while their values are

5

125   presented in table 1. As one can see the two screws have the same pitch (P), the same

126   outer and core radius at their tips (OR_{min}, CR_{min} respectively) and throughout their

127   length they have the same thread depth (D = OR - CR) and thread inclination angles

128   (a_1/a_2). On the contrary the two screws have significantly different conical angles

129   (a_{con}) and as a result of that they also have different outer and core radius at the

130   transition point from the conical to the cylindrical part of the screw (OR_{max}, CR_{max}

131   respectively). From this point on the pedicle screw with $a_{con} = 2.5°$ and $7.0°$ will be

132   referred to as Romeo 2.5 and Romeo 7.0, respectively.

133

134   The conical part of the aforementioned screws were inserted into the SRPF blocks

135   through cylindrical holes that were previously prepared using a pillar drill. The

136   insertion depth of the screws was equal to 20 mm. The radius of the cylindrical holes

137   was equal to the minimum core radius of the screws, that is equal to 1.3 mm.

138

139   The pullout tests were performed following pertinent international experimental

140   standard (ASTM-F543–02) [20] according to which, the SRPF blocks were fixed to

141   the base of the loading frame (MTS Insight 10kN, MTS Systems Corp., Eden Prairie,

142   MN) with the aid of a metallic frame while the screw was suspended from the load

143   cell (MTS 10kN Load Transducer) using a custom-made device (Figure 2). The screw

144   was pulled out of the SRPF block with a constant rate equal to 0.01 mm/s while the

145   respective force was measured with a sampling rate of 10 Hz.

146

147   Ten tests were performed in total (five tests for each screw) to calculate the mean

148   value and the standard deviation of the pullout force, pullout displacement and the

149   corresponding stiffness for each screw. The results for the two screws were compared

150 to each other and their statistical significance was evaluated following one way

151 analysis of variance (ANOVA). The level of statistical significance was considered to

152 be equal to 0.05.

153

154 2.2   FE modelling and validation

155 For the purposes of the present study two different FE models were designed using

156 ANSYS12 software: one FE model for the simulation of under-tapping and

157 cylindrical screw pullout and another one for conical screw pullout. The design of

158 both models was based on the same concept and assumptions.

159

160 The pullout phenomenon was simulated with 2D axisymmetric FE models of a bone

161 screw and of its hosting material. The hosting material of the screw was simulated as

162 a homogenous, isotropic, linearly elastic - perfectly plastic material. Its Young's

163 modulus, yield stress and Poisson's ratio were defined according to the values

164 provided by the manufacturer [21] for the SRPF's compressive modulus, compressive

165 strength and Poisson's ratio respectively (table 2). A preliminary numerical analysis

166 revealed that using the values of the tensile modulus and strength instead of the

167 compressive ones does not affect the value of the screw's pullout force.

168

169 The experimentally observed failure of the synthetic bone was simulated using a

170 technique previously developed for cylindrical screws that are pulled out of SRPF

171 blocks [15]. According to this technique, the FEs which lay in the vicinity of the

172 screw are connected to each other using bonded contact elements (Conta171,

173 Targe169) to form a number of successive areas where failure can occur. The areas of

174 possible failure were cylinders in the case of cylindrical screws (Figure 3) and cones

7

175   in the case of conical screws. Neighbouring elements at opposite sides of the

176   aforementioned surfaces can break apart from one another, should the tangential stress

177   between them exceeds the shear strength of the SRPF.

178

179   A bilinear cohesive zone material model was implemented to control mode-II

180   debonding of neighbouring FEs [18]. According to this model, the tangential stress on

181   the interface between a contact pair rises linearly to a critical value (i.e. the shear

182   strength of the SRPF). Beyond this point, any further increase of the relative sliding

183   causes a non-reversible decrease of the tangential stress leading to the complete

184   debonding of the contact pair. From this point on the interface conditions between the

185   initially bonded pair of elements change to simple contact with friction.

186

187   As far as the macroscopic behaviour of the model is concerned, debonding of

188   neighbouring elements reduces the total force that resists pullout and causes a clear

189   drop of the force in the force/displacement graph. Indeed the force in the numerically

190   calculated force/displacement graph reaches a maximum value and then drops with

191   increasing displacement. The maximum value of the force is stored as the screw's

192   pullout force. Even though the simulation continues beyond the point where the value

193   of the force starts dropping the solution process becomes slower and finally it stops

194   due to non-convergence. In any case the ultimate force, namely the force calculated

195   for the last sub-step of the solution where convergence was achieved, is always lower

196   than the pullout force.

197

198   Taking under consideration the magnitude difference between the Young 's modulus

199   of the screw and of its hosting material, the screw was considered to be rigid [19].

200   Moreover the FE model of the bone screw was designed in a way that enabled the

201   modification of its dimensions and shape. The initial geometry of the screw's FE

202   model was modified to fit inside a cylindrical threaded hole, with dimensions similar

203   to the holes drilled for the pullout testing. In the case of cylindrical screws inserted

204   with under-tapping, the initial core diameter of the screw was modified and set equal

205   to the core diameter of the threaded hole (Figure 4). In the case of conical screws the

206   initial value of the big core diameter of the screw (which is the core diameter of the

207   cylindrical part of the screw) was set equal to the threaded hole's core diameter

208   (Figure 4).

209

210   The simulation was performed in two steps to incorporate the effect of pretension

211   development into the simulation of the pullout phenomenon. During the first step the

212   radii of the FE model of the screw were extended to reach their actual values, while

213   during the second simulation step the screw was pulled out from its hosting material

214   (Figure 4). More specifically during the second load step a displacement was imposed

215   to the screw in the pullout direction with the help of a pilot-node. The value of the

216   imposed displacement was $0.5 \times$ screw's insertion depth. This relatively high

217   displacement value was used to ensure the failure of the screw's hosting material.

218   Indeed the exact value of the imposed displacement has no effect on the calculation of

219   the pullout force. The solution process stops when it reaches a point of non-

220   convergence.

221

222   The accuracy of the numerical analysis was assessed by comparing the numerical

223   results with corresponding experimental ones. For that purpose the FE model of the

224   pullout phenomenon was modified to closely match the geometry, size and insertion

225   depth of the screws that were used for the experiments.

226

227   In the case of cylindrical screws and under-tapping the accuracy of the numerical

228   analysis for was assessed by comparing the numerical results with corresponding

229   experimental ones from a previous investigation performed by authors of this study

230   [4]. Experimental data for two different conditions of under-tapping were used. In the

231   context of that study a cylindrical pedicle screw with core and outer radius equal to

232   2.75 mm and 3.75 mm respectively (CD Horizon Legacy MAS(Ti) 7.5×50 mm,

233   Medtronic Sofamor Danek, Memphis,TN), was pulled out from blocks of synthetic

234   bone with material properties similar to osteoporotic bone (10 pcf SRPF, Sawbones,

235   Worldwide, Pacific Research Laboratories Inc.). Screw insertion was performed with

236   under-tapping. Two different under-tapping ratios were tested, namely the ratio of the

237   screw's core radius divided by the respective radius of the threaded hole (CR^{Screw}

238   $/CR^{TH}$). More specifically the screw was inserted into threaded holes that were

239   smaller than the screw itself by 0.5 mm and 1.0 mm (under-tapping ratios equal to 1.2

240   and 1.6 respectively). The case where the threaded hole had identical size and shape

241   to the screw was also tested (under-tapping ratio 1.0).

242

243   In the case of conical screws, the accuracy of the FE analysis was assessed based on

244   the pullout tests performed in the context of this study for the Romeo 2.5 and Romeo

245   7.0 screws. The experimental force vs. displacement curves and the experimental

246   pullout forces were compared with the respective numerical ones.

247

248

10

249   2.3   Parametric analyses

250

251   After its validation the FE model of cylindrical screw's pullout was utilized to

252   investigate the impact of under-tapping on pullout strength. A cylindrical screw with

253   core and outer radius equal to 2.75 mm and 3.75 mm was simulated inside a

254   cylindrical threaded hole of similar size and shape and its pullout force was calculated

255   for different under-tapping ratios (i.e. CR^{Screw}/CR^{TH}). Starting from an under-tapping

256   ratio of 1 (no under-tapping) the threaded hole's core radius was decreased with

257   increments of 0.1 mm. The parametric investigation was terminated when the results

258   indicated that any further increase of the under-tapping ratio will have no effect to the

259   value of the pullout force. This procedure was repeated for three different SRPF

260   densities: 0.08 g/cc, 0.16 g/cc and 0.24 g/cc. The material properties of these SRPFs

261   were defined according to literature [21] and their values are shown in table 2.

262

263   The FE model of conical screw's pullout was utilized to investigate the impact of

264   conical angle and pretension to pullout strength. The minimum core and minimum

265   outer radius of the screw were kept constant while the respective maximum radii were

266   modified to produce conical threads with different conical angles. Eight different

267   values of the screw's conical angle ranging from $0°$ to $7°$ were simulated. Two different

268   simulations were performed for each one of these conical angles, to quantify the

269   impact of pretension to a conical screw's holding strength. The pretension generated

270   inside the synthetic bone during screw insertion was taken under consideration during

271   the first simulation but excluded from the second one. During the first simulation,

272   pretension generation was simulated by inserting the conical screw inside a

273   cylindrical threaded hole, with core and outer radius similar to the minimum core and

274   outer radius of the screw. On the contrary during the second simulation the conical

275   screws were simulated inside conical threaded holes with size and shape identical to

276   the screw itself. This way no pretension was developed inside the screw's hosting

277   material. The material properties of the screw's hosting material were those of a

278   synthetic bone simulating osteoporotic cancellous bone (10 pcf SRPF, Sawbones,

279   Worldwide, Pacific Research Laboratories Inc.).

280

281   **3.**   **Results**

282

283   3.1   Experimental study

284   All specimens exhibited similar mechanical behaviour and failed under shear. The

285   failure appears on an almost conical surface which connects the edges of the threads

286   of the screw. As it can be seen in figure 5, the failure surface in the case of the Romeo

287   7.0 screw can be described as a cone with conical angle $\approx 7°$, the same as the screw

288   itself. The material between the surface of failure and the surface of the screw is

289   extracted from the block together with the screw. Representative force vs.

290   displacement curves of pullout test are shown in figure 6. The peak value of the force

291   is the screw's pullout force, while the displacement corresponding to this force is the

292   pullout displacement. The tangent of the angle between the linear part of the curve

293   and the X axis corresponds to the stiffness of the screw - screw's hosting material

294   complex. The results of the pullout test are shown in detail in table 3.

295

296   One way ANOVA indicated that Romeo 7.0 screw has statistically significant (P <

297   0.05) higher pullout force than the Romeo 2.5 screw, while there are no statistically

298   significant differences in terms of pullout displacement and stiffness (P > 0.05).

299

300   3.2   FE modelling and validation

301   Figures 6 and 7 depict a clear overview of the simulation process. In the case of

302   cylindrical screws with under-tapping (Figure 6) the screw's radii expand during the

303   first load step, generating a strong and relatively uniform stress field in the vicinity of

304   the screw. During the second load step, the screw is pulled out of its hosting material

305   until failure of the synthetic bone. Debonding is observed in the vicinity of the

306   deepest thread (namely the most distant one from the free surface). Debonding of

307   neighbouring elements generates a sudden stress relief in this region and a

308   discontinuity of the stress field. The strong stress concentration at the edges of the

309   SRPF's free surface are caused by the model's supports (figure 3).

310

311   In the case of conical screw's pullout (Figure 7) the shape of the screw is gradually

312   changed from cylindrical to conical to simulate the generation of pretension around

313   the screw. In this case, the stress field developed in the vicinity of the screw is more

314   severe near the free surface of the SRPF block as expected. During the second load

315   step, the screw is pulled out from its hosting material. Most of the pullout load

316   appears to be carried by the thread closest to the free surface.

317

318   In terms of validation. In the case of under-tapping the experimental/ numerical

319   pullout forces for under-tapping ratios equal to 1.0, 1.2 and 1.6 were 438 N ± 5 N/

320   440 N, 480 N ± 7 N/ 506 N and 481 N ± 9 N/ 505 N respectively. As it can be seen

321   the difference between the numerical simulations and the experiments [4] is less that

322   5% for all three cases. Moreover the FE models were able to simulate the

323   macroscopic response of the SRPF block - bone screw complex to loading.

324   Representative numerical and experimental results are shown in figure 6A for the case

325   of under-tapping ratio equal to 1.2. As it can be seen the numerically calculated force

326   vs. displacement curve appears to be in good agreement with the experimental one.

327

328   The numerically calculated pullout forces for the Romeo 2.5 and Romeo 7.0 screws

329   were equal to 326 N and 381 N respectively. Comparing these values with the

330   respective experimental ones (table 3) gives a difference that is lower than 3%.

331   Moreover, the FE models were able to simulate with satisfactory accuracy the overall

332   response of the SRPF block - bone screw complex (Figure 6B).

333

334

335   3.3   Parametric analyses

336

337   The pullout force calculated for different densities of the synthetic bone and different

338   under-tapping ratios can be seen in figure 9. In the case of the synthetic bone with

339   density equal to 0.08 g/cc , pullout force increased significantly with under-tapping

340   ratios ranging from 1 to 1.12. Indeed the pullout force calculated for under-tapping

341   ratio equal to 1 was 126 N, while for under-tapping ratio equal to 1.12 the pullout

342   force was 143 N, equivalent to 12% increase. Increasing the under-tapping ratio to

343   values greater than 1.12, did not affect the value of the pullout force. The pullout

344   force calculated for under-tapping ratio equal to 1.17 was again 143 N.

345

346   In the case of SRPFs with density equal to 0.16 g/cc and 0.28 g/cc , pullout force

347   increased significantly with under-tapping ratio for ratios up to 1.17 (Figure 9). The

348   pullout force for these two synthetic bones was 440 N and 894 N for under-taping

14

349   ratio equal to 1, while for under-tapping ratio equal to 1.17 pullout force was 507 N

350   and 1048 N respectively, equivalent to 15% and 17% increase respectively. Increasing

351   the under-tapping ratio to 1.22 had no significant effect to the values of the pullout

352   force (Figure 9). The pullout force calculated for synthetic bones of densities equal to

353   0.16 g/cc and 0.28 g/cc and under-tapping ratio equal to 1.22 was 506 N and 1050 N

354   respectively.

355

356   The pullout force calculated for different values of the conical angle can be seen in

357   figure 10A, for the cases where initial pretension is either included or excluded from

358   the numerical simulation. As it can be noticed, pullout force increases linearly with

359   conical angle when no pretension phenomena are included to the analysis. On the

360   contrary when pretension is included to the numerical simulation the increase is non-

361   linear. The pullout forces calculated in this case are higher than the respective ones

362   calculated without any pretension. Comparing the results for these two series of

363   simulations indicates that pretension has a positive effect on screw pullout strength

364   (Figure 10B). The maximum impact of pretension was calculated for a conical angle

365   equal to 2°. In this case pretension improved the screw's pullout strength by 11.4%.

366   The benefit of pretension on pullout strength becomes weaker for conical angles

367   greater than 2°. Indeed for conical angle equal to 7° pretension causes only a 0.4%

368   increase of the pullout force.

369

370

371

372

373

4.   Discussion and conclusions

It is well established in literature that the stress developed around a bone screw during insertion can significantly influence its stability [4-6, 8-13, 22]. More specifically, it is indicated that the fixation strength of a bone screw can be improved by under-tapping [4-6] or the use of screws with conical core [8-13]. In the case of under-tapping a cylindrical screw is inserted into a previously opened threaded hole which is smaller than the screw itself. In this case the core of the screw compresses and compacts the bone which lies in its vicinity in the radial direction. The core diameter of the threaded hole is expanded until it becomes equal to the diameter of the screw core. The strong contact pressure that is generated on the interface between the cores of the screw and the threaded hole, also generate frictional forces which resist screw's rotation. If the screw is a self-tapping one then its threads will cut their way through the hosting material of the screw. In this case the pressure field developed on the surface of the threads would be relatively weak.

On the other hand, screws with conical core are inserted into bone using previously opened cylindrical holes. In this case screw insertion causes the core of the hole to change size and shape. The shape of the hole changes from cylindrical to conical causing the screw's hosting material near the screw's insertion site to be compressed more than the material near the screw's tip.

Despite its significance, the pretension that is developed during screw insertion has not yet been fully incorporated into FE simulations of screw pullout. Hsu, Chao et al. [8, 9] were the first who tried to simulate the impact of inserting a conical screw into a

16

399 cylindrical hole to the screws pullout strength. Their simulation was based on the idea

400 that the material properties of a screw's hosting material are altered in the vicinity of

401 the screw as a result of material compaction. The main limitations of this approach is

402 the fact that the effect of bone compaction is predefined and that the actual pullout

403 force is not calculated.

404

405 Indeed, assuming that the elastic modulus of the screw's hosting material is a function

406 of volume reduction means that screw fixation strength will continuously increase

407 with compaction. On the other hand there is strong evidence in the literature that

408 fixation strength increases with compaction only up to a certain level [4, 23, 24].

409

410 The impact of the relative dimensions of screw and hole to the screw's pullout

411 strength was investigated experimentally by authors of the present study [4]. A

412 cylindrical pedicle screw was inserted into blocks of synthetic bone using threaded

413 and cylindrical holes of different sizes and the pullout force was measured. The

414 results indicated that there is an optimum ratio of the threaded or cylindrical hole's

415 radius over the respective screw's radius.

416

417 The FE model of Hsu, Chao et al. [8, 9] was capable of calculating the reaction force

418 for a small value of imposed displacement. The value of the reaction force for a

419 constant value of pullout displacement is directly correlated to the stiffness of the

420 screw - hosting material complex rather to the screw's pullout force. According to

421 literature [11, 25-30] and also according to the respective international experimental

422 standard [20] the most appropriate way to quantify the fixation strength of a bone

423 screw is to measure its pullout force.

424

425   In this context the present study's aim was to establish a new method for simulating

426   the pretension that is developed inside the hosting material of a screw during screw

427   insertion and to incorporate it in the numerical simulation of the pullout phenomenon.

428   The screw was simulated inside a cylindrical threaded hole with dimensions similar to

429   the holes drilled for pullout testing. The initial dimensions of the screw's FE model

430   were modified to match the dimensions of the cylindrical threaded hole. The

431   simulation was performed in two steps: 1) Pretension generation, 2) pullout. Preten-

432   sion generation was simulated by extending the screw's radii to reach their actual

433   values. After the completion of this load step a displacement at the pullout direction

434   was imposed to the screw until the failure of its hosting material.

435

436   The experimentally observed failure of the synthetic bone was simulated by

437   implementing a bilinear cohesive material model [18]. This methodology has been

438   proven to give reliable estimations of the pullout force of cylindrical screws that are

439   inserted into blocks of synthetic bone through cylindrical threaded holes of identical

440   size and shape to the screw itself [15]. The main limitation of this approach for the

441   simulation of synthetic bone's failure is that the geometrical domain where failure can

442   occur has to be known in advance [16].

443

444   For cylindrical screws that are inserted with under-tapping into blocks of synthetic

445   bone it has been proven previously that failure occurs on a cylindrical surface that

446   includes the screw [4, 15]. Moreover for the case of conical screws it was proven here

447   that failure occurs on a conical surface which includes the screw. These experimental

448   observations indicate that in both cases the screw's hosting material fails under shear

449 and that both are eligible for using a cohesive material model to simulate synthetic

450 bone failure.

451

452 The accuracy of this FE model was validated by comparing the numerically calculated

453 force vs. displacement curves and also the values of the pullout force with

454 experimental ones for two different cases of under-tapping ratios and for two different

455 conical screws. This comparison indicated that the proposed methodology for

456 introducing pretension in the simulation of conical screw pullout enables the accurate

457 assessment of its pullout strength.

458

459 After validation two different parametric analyses were performed. The results of the

460 first parametric study demonstrated that under tapping can significantly increase the

461 pullout force of bone screws. Indeed the impact of under tapping is more pronounced

462 in the case of denser and "stronger" synthetic bones. More specifically under tapping

463 was able to increase pullout force up to 12%, 15% and 17% in the cases of synthetic

464 bones with density equal to 0.08 g/cc, 0.16 g/cc and 0.28 g/cc respectively. Moreover

465 an optimum value of the under tapping ratio exists which appears to be influenced by

466 the mechanical properties of the screw's hosting material. Increasing the under

467 tapping ratio beyond this value has no significant effect on the screw's pullout force.

468

469 In the context of the second parametric analysis the minimum core and outer radii of a

470 conical screw were kept constant while the maximum ones were modified to produce

471 different conical angles. According to literature the outer radius of a screw is one of

472 the most important parameters for its fixation strength. Indeed a screw's pullout force

473 increases linearly with its outer radius [15, 31-33]. For the purpose of this study the

19

474   impact of pretension was quantified separately from that of the maximum outer

475   radius.

476

477   The results of this parametric analysis indicated that using a bone screw with a conical

478   core generates a pretension inside the screw's hosting material which can improve the

479   screw's fixation strength. The impact of the pretension to the screw's fixation strength

480   appears to be stronger for relatively small conical angles. Indeed for a conical angle

481   equal to $2°$, 11.4% of the screw's pullout force is attributed to the pretension

482   generated during screw insertion. On the other hand in the case of a screw with

483   conical angle equal to $7°$ only a 0.4% of its pullout force is a result of pretension.

484

485   Based on the above it could be deduced that in the case of conical screws with big

486   conical angles the best way to improve their short-term fixation strength would be to

487   insert them into conical holes instead of cylindrical ones. The conical angles of these

488   holes should be a couple of degrees smaller than the screw's itself. A possible way to

489   open a conical hole that is smaller than the screw could be to use another screw of

490   similar shape but smaller in size. In a previous experimental investigation performed

491   by authors of the present study it was concluded that using a self-tapping screw to

492   prepare a threaded hole can be as efficient as if a tap was used [4].

493

494   The main limitation of the present study stems from the fact that synthetic bone

495   cannot simulate all aspects of the mechanical behaviour of cancelous bone.

496   Nevertheless synthetic bone can be used to perform comparative analyses and draw

497   useful and clinically relevant conclusions [34]. One of the important aspects of bone

498   tissue that cannot be simulated using synthetic bone is the tissues adaptive response to

20

499   loading. For this reason the results of this study in terms of fixation strength

500   correspond to the first post-operative weeks.

501

502   At this point is should be stressed out that the accuracy of the novel technique

503   proposed here for the simulation of pretension has been validated only for the case of

504   a synthetic bone with density equal to 0.16 g/cc. As a result of that interpreting the

505   numerical results for surrogate bones of different densities should be done with

506   caution. Indeed the FE analyses can predict the maximum possible pretension-induced

507   improvement of a screw's pullout strength. The main prerequisite for this prediction to

508   be accurate is that the screw's hosting material fails during pullout under shear and not

509   during screw insertion. Unfortunately under-tapping also carries the risk of a

510   catastrophic failure during screw insertion [35]. Moreover it is possible that in the

511   case of SRPFs that are denser than 0.16 g/cc an 'under-tapping limit' exists beyond

512   which the integrity of the screw's hosting material is jeopardised during screw

513   insertion. The simulation of this type of failure was beyond the scope of the present

514   study.

515

516   According to literature under-tapping can lead to pedicle wall breach [35].

517   Investigating numerically the possibility of pedicle wall breach requires an accurate

518   simulation of the three-dimensional (3D) geometry of the vertebra and of the screw.

519   Investigating the impact of vertebral 3D geometry was beyond the scope of the

520   present study and therefore the geometry of the screw and of its hosting material was

521   simplified.

522

523   On the other hand the main contribution of the present study is the implementation of

524   a novel method for incorporating the impact of different screw insertion techniques

525   and pretension to the FE simulation of the pullout phenomenon.

526

527

528

529

530

531

532

533

534

535

536

537

538

539

540

541

542

543

544

545

546

547

References:

[1] Okuda S, Miyauchi A, Oda T, Haku T, Yamamoto T, Iwasaki M. Surgical complications of posterior lumbar interbody fusion with total facetectomy in 251 patients. J Neurosurg Spine. 2006;4:304-9.

[2] Esses SI, Sachs BL, Dreyzin V. Complications associated with the technique of pedicle screw fixation. A selected survey of ABS members. Spine (Phila Pa 1976). 1993;18:2231-8; discussion 8-9.

[3] Ponnusamy KE, Iyer S, Gupta G, Khanna AJ. Instrumentation of the osteoporotic spine: biomechanical and clinical considerations. Spine J. 2011;11:54-63.

[4] Chatzistergos PE, Sapkas G, Kourkoulis SK. The Influence of the Insertion Technique on the Pullout Force of Pedicle Screws An Experimental Study. Spine. 2010;35:E332-E7.

[5] Halvorson TL, Kelley LA, Thomas KA, Whitecloud TS, 3rd, Cook SD. Effects of bone mineral density on pedicle screw fixation. Spine (Phila Pa 1976). 1994;19:2415-20.

[6] Kuklo TR, Lehman RA, Jr. Effect of various tapping diameters on insertion of thoracic pedicle screws: a biomechanical analysis. Spine (Phila Pa 1976). 2003;28:2066-71.

[7] Wu Z, Nassar SA, Yang X. Pullout performance of self-tapping medical screws. J Biomech Eng. 2011;133:111002.

[8] Hsu CC, Chao CK, Wang JL, Hou SM, Tsai YT, Lin J. Increase of pullout strength of spinal pedicle screws with conical core: biomechanical tests and finite element analyses. J Orthop Res. 2005;23:788-94.

572 [9] Chao CK, Hsu CC, Wang JL, Lin J. Increasing bending strength and pullout

573 strength in conical pedicle screws: biomechanical tests and finite element analyses. J

574 Spinal Disord Tech. 2008;21:130-8.

575 [10] Abshire BB, McLain RF, Valdevit A, Kambic HE. Characteristics of pullout

576 failure in conical and cylindrical pedicle screws after full insertion and back-out.

577 Spine J. 2001;1:408-14.

578 [11] Kwok AW, Finkelstein JA, Woodside T, Hearn TC, Hu RW. Insertional torque

579 and pull-out strengths of conical and cylindrical pedicle screws in cadaveric bone.

580 Spine (Phila Pa 1976). 1996;21:2429-34.

581 [12] Kim YY, Choi WS, Rhyu KW. Assessment of pedicle screw pullout strength

582 based on various screw designs and bone densities-an ex vivo biomechanical study.

583 Spine J. 2012;12:164-8.

584 [13] Krenn MH, Piotrowski WP, Penzkofer R, Augat P. Influence of thread design on

585 pedicle screw fixation. Laboratory investigation. J Neurosurg Spine. 2008;9:90-5.

586 [14] Janssen D, Zwartele RE, Doets HC, Verdonschot N. Computational assessment

587 of press-fit acetabular implant fixation: the effect of implant design, interference fit,

588 bone quality, and frictional properties. Proc IMechE 2009;224:67-75.

589 [15] Chatzistergos PE, Magnissalis EA, Kourkoulis SK. A parametric study of

590 cylindrical pedicle screw design implications on the pullout performance using an

591 experimentally validated finite-element model. Med Eng Phys. 2010;32:145-54.

592 [16] Feerick EM, McGarry JP. Cortical bone failure mechanisms during screw

593 pullout. J Biomech. 2012;45:1666-72.

594 [17] Feerick EM, Liu XC, McGarry P. Anisotropic mode-dependent damage of

595 cortical bone using the extended finite element method (XFEM). J Mech Behav

596 Biomed Mater. 2013;20:77-89.

597 [18] Alfano G, Crisfield MA. Finite element interface models for the delamination

598 analysis of laminated composites: Mechanical and computational issues. International

599 Journal for Numerical Methods in Engineering. 2001;50:1701-36.

600 [19] Chatzistergos PE, Spyrou CE, Magnissalis EA, Kourkoulis SK. Dependence of

601 the pullout behaviour of pedicle screws on the screw - hosting material relative

602 deformability. International Journal of Computer Aided Engineering and Technology.

603 2013;5:343-61.

604 [20] ASTM. **F 543 – 02** Standard Specification and Test Methods for Metallic Medical

605 Bone Screws. Medical Device Standards and Implant Standards2004.

606 [21] Sawbones.2013.Sawbones webpage,http://www.sawbones.com/.

607 [22] Silva P, Rosa RC, Shimano AC, Defino HL. Effect of pilot hole on

608 biomechanical and in vivo pedicle screw-bone interface. Eur Spine J. 2013.

609 [23] Steeves M, Stone C, Mogaard J, Byrne S. How pilot-hole size affects bone-screw

610 pullout strength in human cadaveric cancellous bone. Can J Surg. 2005;48:207-12.

611 [24] Ansell RH, Scales JT. A study of some factors which affect the strength of

612 screws and their insertion and holding power in bone. J Biomech. 1968;1:279-302.

613 [25] Hitchon PW, Brenton MD, Coppes JK, From AM, Torner JC. Factors affecting

614 the pullout strength of self-drilling and self-tapping anterior cervical screws. Spine

615 (Phila Pa 1976). 2003;28:9-13.

616 [26] Leggon R, Lindsey RW, Doherty BJ, Alexander J, Noble P. The holding strength

617 of cannulated screws compared with solid core screws in cortical and cancellous

618 bone. J Orthop Trauma. 1993;7:450-7.

619 [27] Lyon WF, Cochran JR, Smith L. Actual Holding Power of Various Screws in

620 Bone. Ann Surg. 1941;114:376-84.

621 [28] Pfeiffer FM, Abernathie DL, Smith DE. A comparison of pullout strength for

622 pedicle screws of different designs: a study using tapped and untapped pilot holes.

623 Spine (Phila Pa 1976). 2006;31:E867-70.

624 [29] Reitman CA, Nguyen L, Fogel GR. Biomechanical evaluation of relationship of

625 screw pullout strength, insertional torque, and bone mineral density in the cervical

626 spine. J Spinal Disord Tech. 2004;17:306-11.

627 [30] Wittenberg RH, Lee KS, Shea M, White AA, 3rd, Hayes WC. Effect of screw

628 diameter, insertion technique, and bone cement augmentation of pedicular screw

629 fixation strength. Clin Orthop Relat Res. 1993:278-87.

630 [31] Asnis SE, Ernberg JJ, Bostrom MP, Wright TM, Harrington RM, Tencer A, et al.

631 Cancellous bone screw thread design and holding power. J Orthop Trauma.

632 1996;10:462-9.

633 [32] DeCoster TA, Heetderks DB, Downey DJ, Ferries JS, Jones W. Optimizing bone

634 screw pullout force. J Orthop Trauma. 1990;4:169-74.

635 [33] Gausepohl T, Mohring R, Pennig D, Koebke J. Fine thread versus coarse thread.

636 A comparison of the maximum holding power. Injury. 2001;32 Suppl 4:SD1-7.

637 [34] Schoenfeld AJ, Battula S, Sahai V, Vrabec GA, Corman S, Burton L, et al.

638 Pullout strength and load to failure properties of self-tapping cortical screws in

639 synthetic and cadaveric environments representative of healthy and osteoporotic bone.

640 J Trauma. 2008;64:1302-7.

641 [35] Chin KR, Gibson B. The risks of pedicle wall breech with larger screws after

642 undertapping. Spine J. 2007;7:570-4.

643

644

Tables:

Table 1: The geometrical quantities that describe the geometry of the threads of Romeo 2.5 and Romeo 7.0 screw.

Screw	P (mm)	D (mm)	OR_{min} (mm)	CR_{min} (mm)	a_{con} (deg)	OR_{max} (mm)	CR_{max} (mm)	a_1/a_2 (deg)
Romeo 2.5	2.8	0.8	2.1	1.3	2.5	2.9	2.1	5/20
Romeo 7.0					7.0	3.7	4.5	

Table 2: The material properties of three different SRPFs used for the parametric study of under-tapping impact on screw pullout (Sawbones, Worldwide, Pacific Research Laboratories Inc.) [21].

Density (g/cc)	Compressive Strength (MPa)	Compressive Modulus (MPa)	Shear Strength (MPa)	Poisson's ratio
0.08	0.6	16	0.59	
0.16	2.2	58	1.6	0.3
0.24	4.9	123	2.8	

Table 3: The pullout force, pullout displacement and stiffness measured for the Romeo 7.0 and the Romeo 2.5 screw. The respective numerical values are given in brackets for comparison.

	Romeo 7.0			Romeo 2.5		
	Force (N)	Displacement (mm)	Stiffness (N/mm)	Force (N)	Displacement (mm)	Stiffness (N/mm)
a	*385*	*0.83*	*543*	*315*	*0.82*	*433*
b	*393*	*0.86*	*558*	*324*	*0.67*	*580*
c	*379*	*0.85*	*558*	*317*	*0.70*	*536*
d	*391*	*0.88*	*538*	*321*	*0.86*	*443*
e	*376*	*0.89*	*507*	*312*	*0.75*	*476*
Mean	385(*381*)	0.86(*0.80*)	541(*582*)	318(*326*)	0.76(*0.76*)	494(*517*)
STDEV	7	0.02	21	5	0.08	63

27

Figure captions:

660

661   Fig. 1: The pedicle screws used for the realization of the pullout tests (up) and the

662   basic geometrical features of the conical pedicle screws used (down).

663

664   Fig. 2: Schematic representation of the experimental set-up.

665

666   Fig. 3: The FE model of a cylindrical screw's hosting material for the case where

667   screw insertion is performed with under-tapping.

668

669   Fig. 4: The two load steps realized in the case of under-tapping (up) or conical screws

670   (down) to assess the impact of pretension to pullout strength: Pretension development

671   (left) and pullout (right).

672

673   Fig. 5: A central section of an SRPF block after the completion of a pullout test. The

674   test was performed using the Romeo 7.0 screw. The section was pressed against a

675   carbon paper to make the conical hole caused by screw pullout easily distinguishable.

676

677   Fig. 6: The experimentally measured and the numerically estimated force vs.

678   displacement curves for cylindrical screw with under-tapping ratio equal to 1.2 (A)

679   and for the conical screws Romeo 2.5 and Romeo 7.0 (B). For each case the

680   experimental curves correspond to the tests which gave the maximum and minimum

681   pullout force.

682

683

684   Fig. 7: The distribution of the Von Mises equivalent stress (Pa) during different stages

685   of the simulation of pretension generation (left) and pullout (right) for a cylindrical

686   screw that is inserted with under-tapping.

687

688   Fig. 8: The distribution of the Von Mises equivalent stress (Pa) during different stages

689   of the simulation of pretension generation (left) and pullout (right) for a conical screw

690   that is inserted into a cylindrical threaded hole.

691

692   Fig. 9: The numerically calculated pullout force vs. under-tapping ratio for three

693   different densities of synthetic bone.

694

695   Fig. 10: The pullout force calculated for different conical angles for the cases where

696   initial pretension is included or not to the numerical simulation (A) and the %

697   difference between these two cases (B).

698

699

700

701

702

703

704

705

706

707

708

709   Figure 1:

710
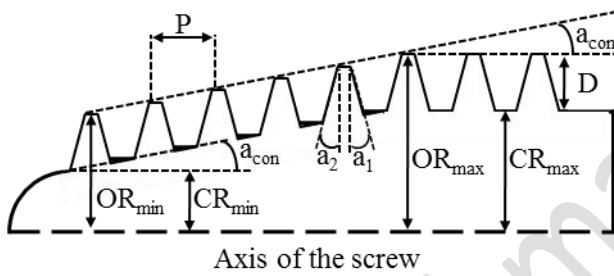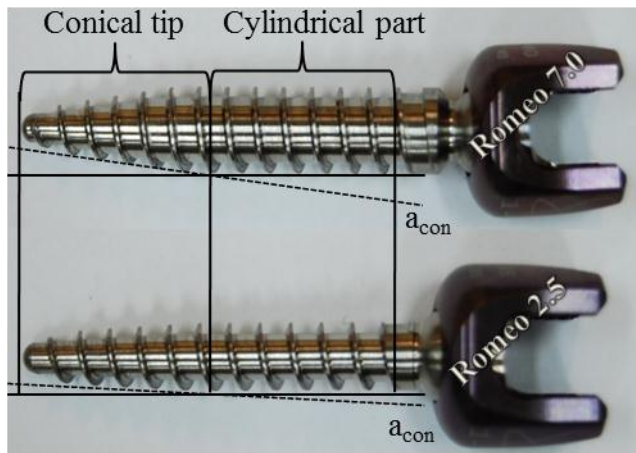
711

712

713

714

715

716

717

718

719

720

721

722

723

724

725   Figure 2:

726

Load cell

Pedicle
screw

SRPF block
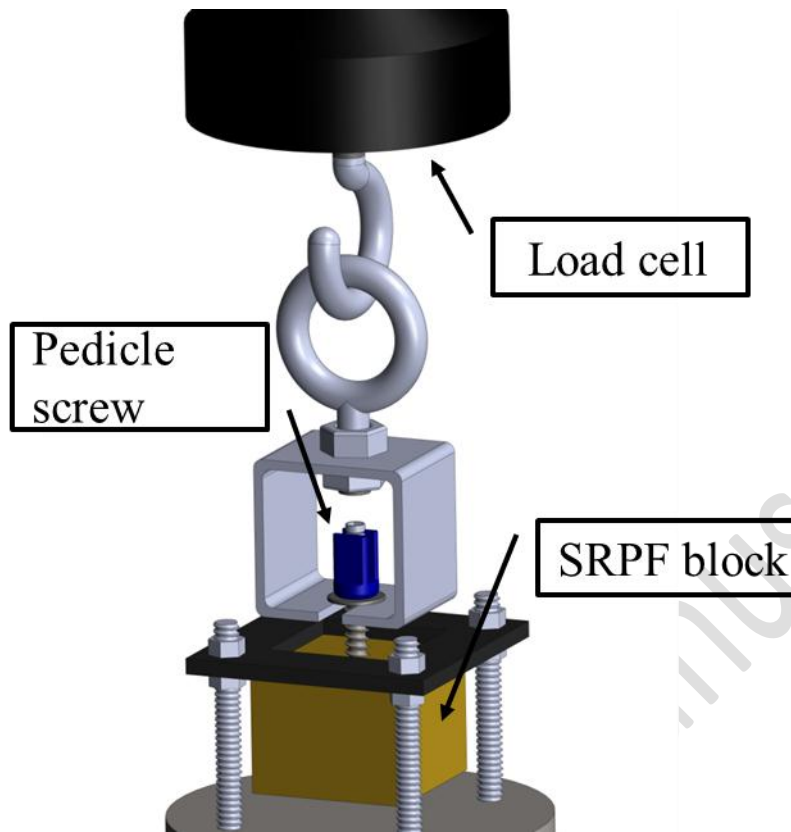
727

728

729

730

731

732

733

734

735

736

737

738

739

740   Figure 3:

741
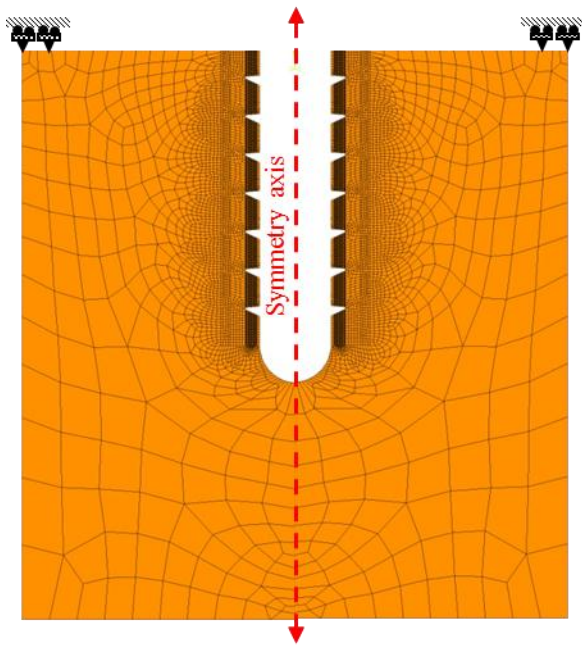
742

743

744

745

746
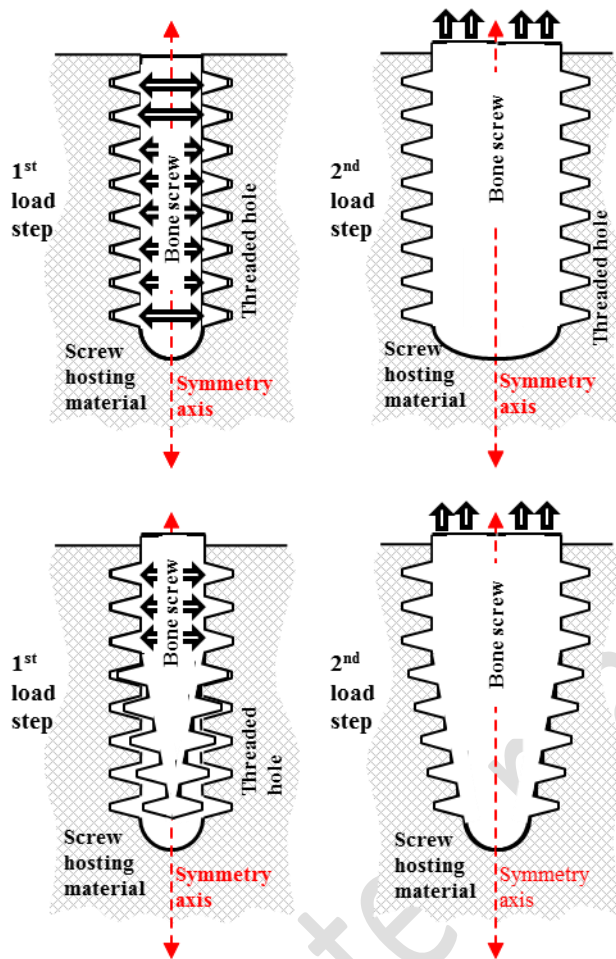
747

748

749

750

751

752

753

754

755

756

757

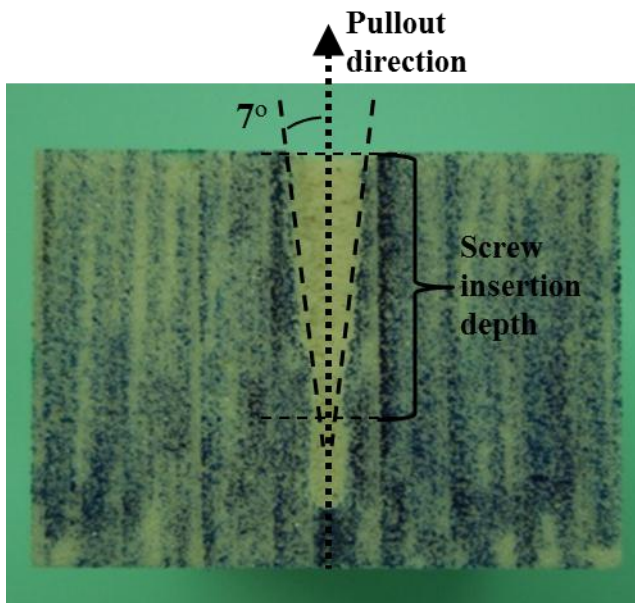758 Figure 4:

759

760

761

762

763

764

765

766

767

768

769

770

771   Figure 5:
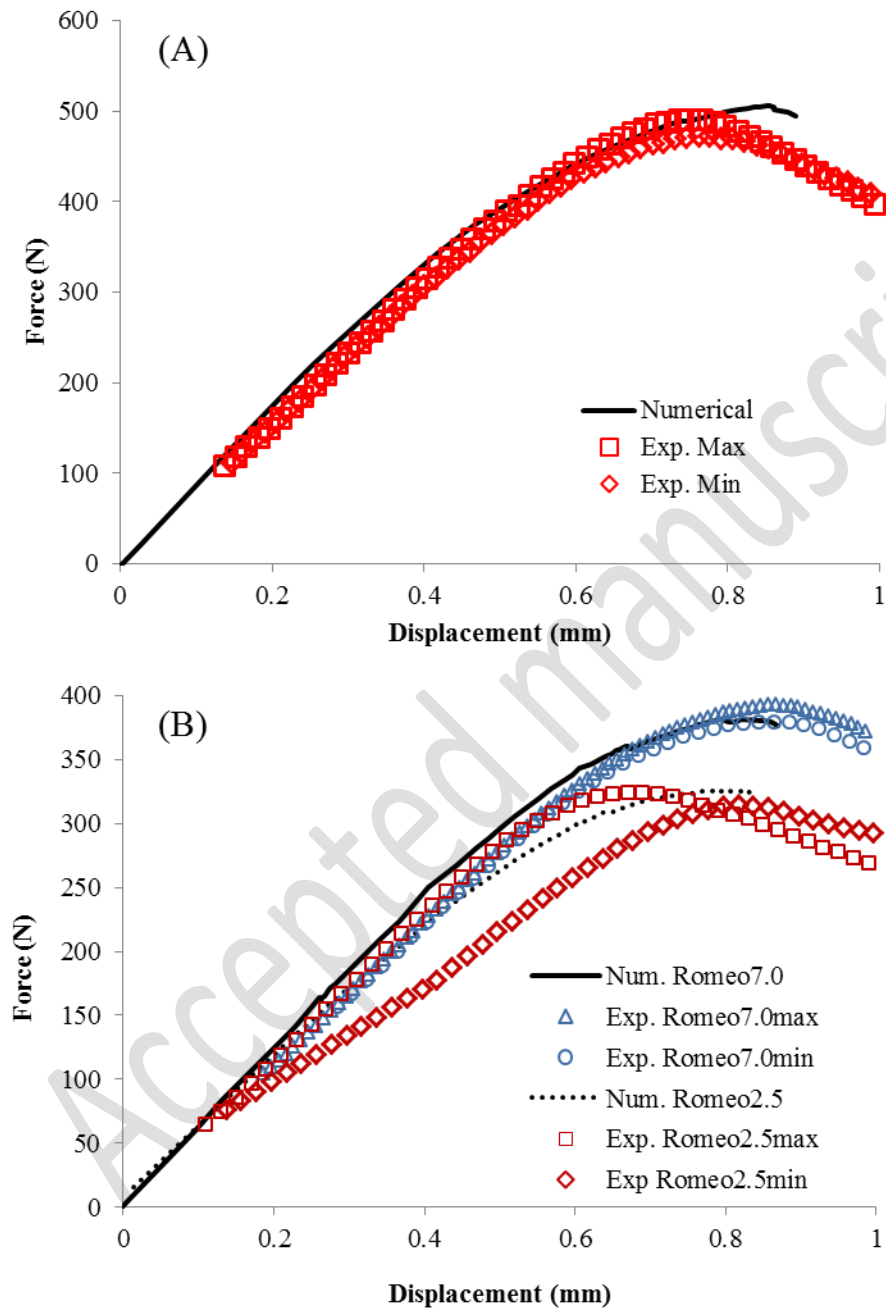
772

773

774

775

776

777

778

779

780

781

782

783

784

785

786

787

788

789   Figure 6:

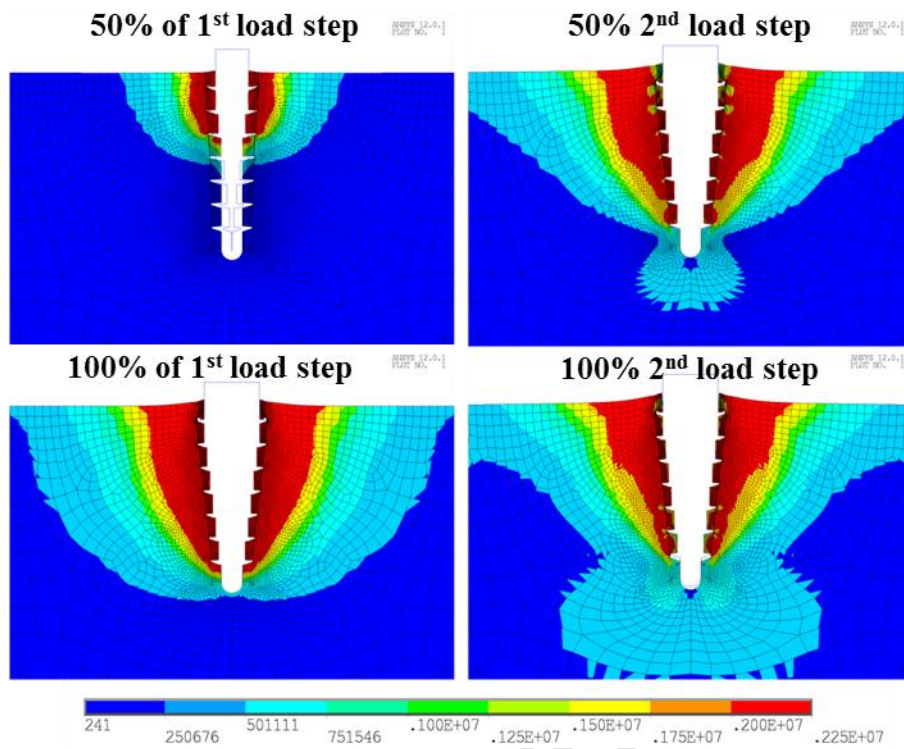790

791

792

793

794

795

796   Figure 7:

797

50% of 1st load step   50% 2nd load step

100% of 1st load step   100% 2nd load step
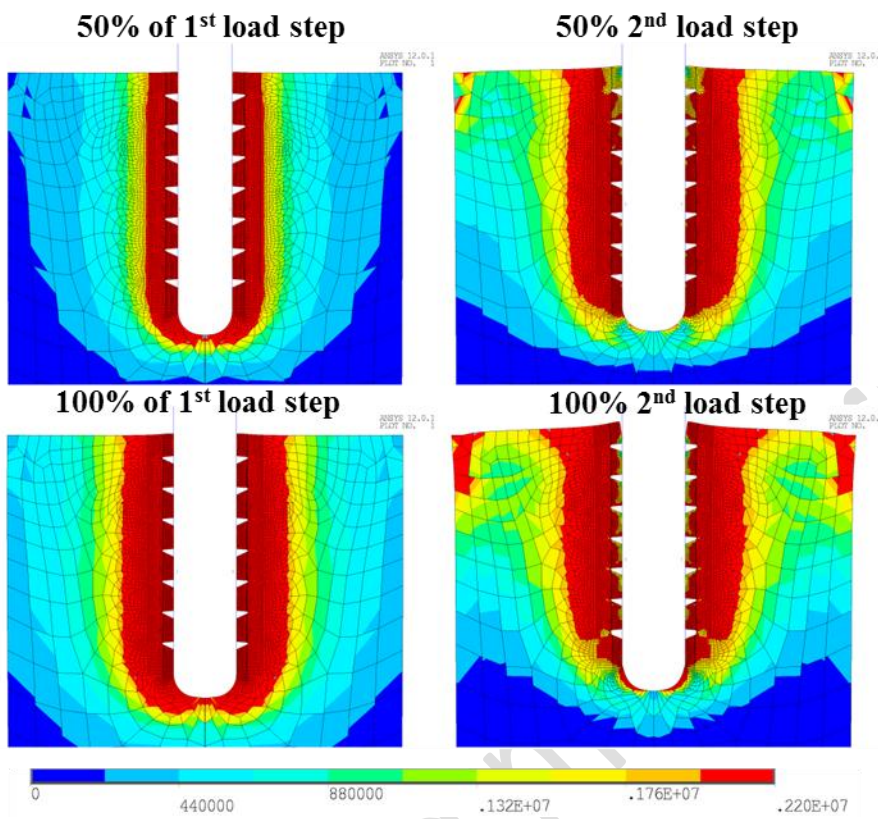
798

799

800

801

802

803

804

805

806

807

808

809

810

811   Figure 8:

812

813

814

815

816

817

818
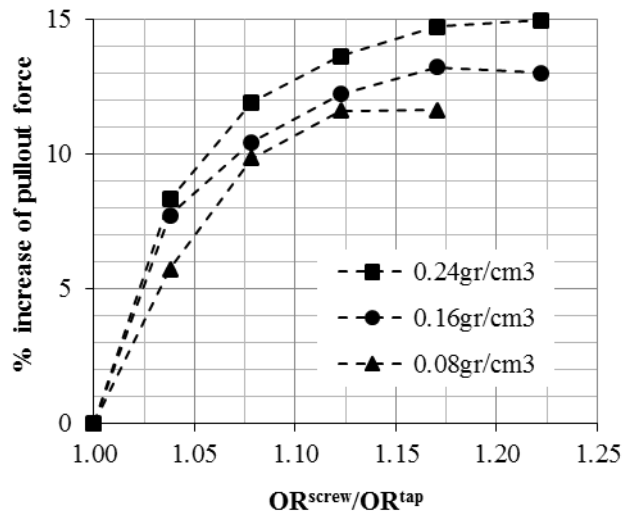
819

820

821

822

823

824

825

826

827   Figure 9:

828

829

830

831

832

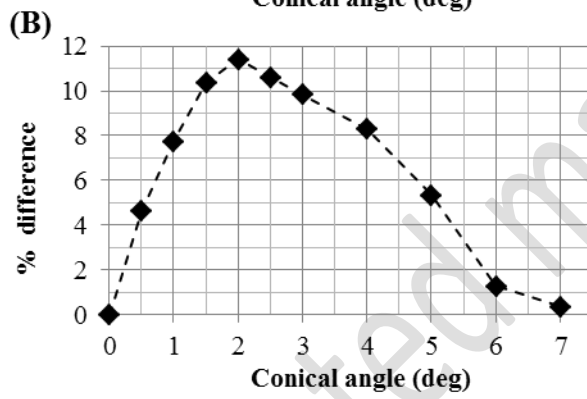833

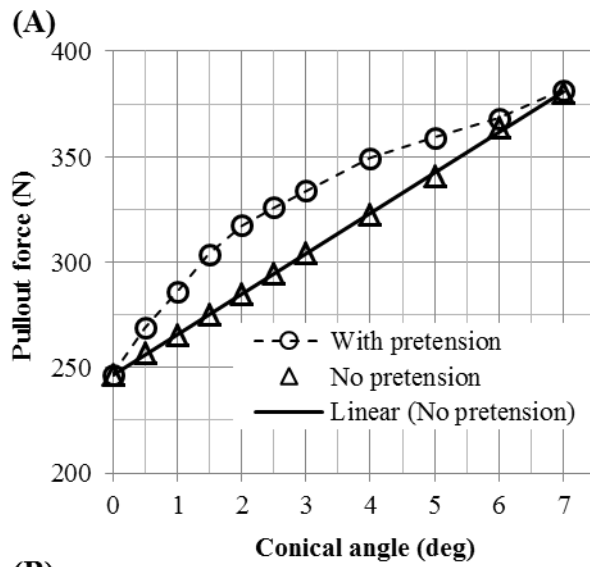834

835

836

837

838

839

840

841

842

843

844

845

846

847   Figure 10:

848

(A) Pullout force (N) vs. Conical angle (deg) with legend: With pretension, No pretension, Linear (No pretension)

(B) % difference vs. Conical angle (deg)

849

850